

## Preparation and characterization of Eu doped zirconia luminescent films synthesized by the pyrosol technique

M. GARCIA-HIPOLITO

*Programa de Posgrado en Tecnología Avanzada, CICATA-IPN, Legaria, México, DF*

E. MARTINEZ, O. ALVAREZ-FREGOSO

*Instituto de Investigaciones en Materiales, UNAM, A.P. 70-360 Coyoacán 04510 México, DF*

*E-mail: oaf@seridor.unam.mx*

C. FALCONY

*Departamento de Física, CINVESTAV-IPN, Apdo. Postal 14-740, México D F. 07000. (In sabbatical leave at Dep. of Materials Science, ESFM-IPN)*

M. A. AGUILAR-FRUTIS

*Centro de Investigación en Ciencia Aplicada y Tecnología Avanzada, CICATA-IPN, Legaria, México, DF*

The pyrosol method is a well-known process for depositing films [1, 2]. The main advantages of this technique are its low cost, a high deposition rate, the possibility to coat large areas, its ease of operation and the quality of the coatings obtained. This technique has been used to deposit successfully a variety of films such as oxides, sulfides and metals [1]. Zirconia has attracted much attention in science and technology because its high melting temperature, high refractive index, low thermal conductivity, hardness and corrosion barrier properties [3]. Furthermore these films are useful in corrosion resistance applications [4], as insulating layers in very large scale integrated (VLSI) circuits [5], for optical coatings [6], in buffer layers for high  $T_c$  oxide superconductors [7], etc. There are also some studies on rare earth doped luminescent zirconia single crystals and powders [8–10]. The present contribution is devoted to the preparation and characterization of  $ZrO_2:Eu$  photoluminescent (PL) and cathodoluminescent (CL) films synthesized by the pyrosol technique. To our best knowledge, there has been no report on luminescent coatings of  $ZrO_2:Eu$ . These films can be applied in cathode ray tubes; color plasma displays panels, fluorescent lamps, vacuum fluorescent display devices and electroluminescent flat panel displays.

The experimental arrangement for pyrosol technique has been presented elsewhere (2). The spraying solution was 0.05 M solution of zirconium oxychloride ( $ZrOCl_2 \cdot 8H_2O$ , Merck) in deionized water. Doping with Eu was achieved by adding  $EuCl_3 \cdot 6H_2O$  to the spraying solution in the range from 1 to 20 atomic percent (a/o) in relation to the Zr content in this solution. The carrier gas flow (filtered air) was 10 liter/min. The substrate temperature ( $T_s$ ) during deposition was in the range from 250 to 500 °C; the substrates used were fused quartz slides and (100) n-type silicon single crystals. The deposition time was adjusted (5–8 min) to get similar thickness on all samples studied. This thickness was approximately

5  $\mu m$  as measured by a Sloan Dektak IIA stylus-type recording profilometer. The crystalline structure of the deposited films was analyzed by X-ray diffraction (XRD), using a Siemens D-5000 diffractometer ( $\lambda = 1.5406 \text{ \AA}$  Cu  $k_\alpha$ ). The chemical composition of the films was measured using energy dispersive spectroscopy (EDS) with a Leica-Cambridge electron microscope Mo. Stereoscan 440. The excitation (PLE) and emission PL spectra were obtained using a Perkin-Elmer LS50B fluorescence spectrophotometer. CL measurements were performed in a stainless steel vacuum chamber with a cold cathode electron gun (Luminoscope, model ELM-2 MCA, Relion Co.). The emitted light from the sample was coupled into an optical fiber bundle leading to the spectrophotometer cited above.

Results from X-ray diffractometry of the samples are shown in the Fig. 1. In this case, diffractograms for sample  $ZrO_2:Eu$  (20 a/o in solution) prepared at  $T_s$  from 250 to 500 °C are presented. The  $ZrO_2:Eu$  coatings

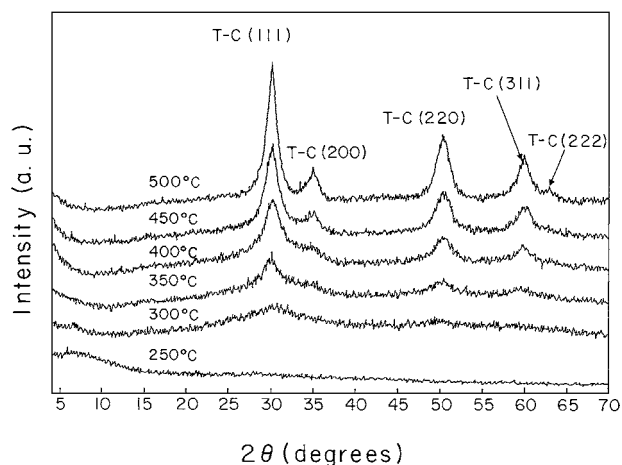


Figure 1 X-ray diffraction patterns for  $ZrO_2:Eu^{3+}$  films at six different deposition temperatures, 250, 300, 350, 400, 450 and 500 °C. (T = tetragonal zirconia, C = cubic zirconia).

TABLE I Atomic percent content of the oxygen, zirconium, europium and chlorine in the  $ZrO_2:Eu^{3+}$  films as measured by EDS for different  $EuCl_3$  concentrations in the spraying solution

$EuCl_3$ concentration in the spraying solution (a/o)	Oxygen	Zirconium	Europium	Chlorine
0	64.69	34.06	00.00	01.25
1	64.08	33.76	00.35	01.81
3	62.97	33.61	00.93	02.49
5	62.81	32.85	01.28	03.06
10	62.43	31.53	02.16	03.88
20	61.62	29.39	03.67	05.32

$T_s = 500^\circ C$ .

remain in the non-crystalline state when deposited at  $T_s$  up to  $350^\circ C$ , but when the  $T_s$  is increased above this value, various peaks associated to a metastable tetragonal or cubic zirconia crystalline phase appear. Increasing  $T_s$  promotes the growth of crystalline material with a preferential orientation on the (111) direction normal to the films surface and an increase in the crystallite size.

EDS measurements were performed on films deposited on single crystals silicon substrates in order to evaluate the oxygen content in the films. The obtained results are shown in Tables I and II. Table I summarizes the relative chemical content of the oxygen, zirconium, europium and chlorine present into the films as a function of the content of the  $EuCl_3$  inserted in the spraying solution. A reduction of the relative content of oxygen and zirconium and, furthermore, an increase in the relative contents of europium and chlorine is observed when the doping concentration rises. The  $T_s$ , in this case, was  $500^\circ C$ . Table II presents results similar to those in Table I but as a function of the  $T_s$ , keeping constant the doping concentration ( $EuCl_3$ , 5 a/o) in the starting solution. Here, we observe an increase in the content of oxygen and a reduction in the content of zirconium, europium and chlorine as the  $T_s$  increases.

Fig. 2 shows an excitation spectrum for the 612 nm emission from a sample deposited at  $T_s = 500^\circ C$  and 5 a/o (in the spraying solution) of activator concentration. This spectrum consist of a broad band ranging from 220 to 400 nm ( $\lambda_{max} = 257$  nm), corresponding to transitions within the  $4f^6$  configuration of  $Eu^{3+}$  and of the  $O^{2-}-Eu^{3+}$  charge transfer excitation band (CTB).

The emission spectra (using  $\lambda_{ex} = 257$  nm), as a function of concentration activator are shown in the Fig. 3.

TABLE II Atomic percent content of the oxygen, zirconium, europium and chlorine in the  $ZrO_2:Eu^{3+}$  films as determined by EDS for different  $T_s$

Substrate temperature ( $^\circ C$ )	Oxygen	Zirconium	Europium	Chlorine
250	50.29	36.34	05.01	08.36
300	52.18	35.83	04.17	07.82
350	55.29	34.96	03.40	06.35
400	57.03	34.65	02.98	05.34
450	60.68	33.09	02.05	04.18
500	62.81	32.85	01.28	03.06

$EuCl_3$  concentration in the spraying solution was 5 a/o.

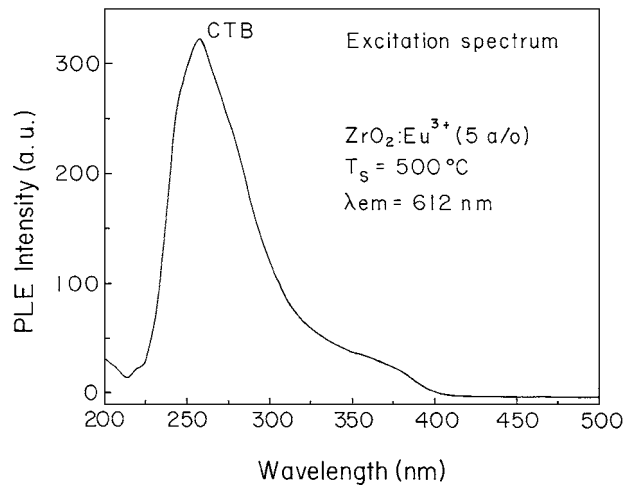


Figure 2 Excitation spectrum from  $ZrO_2:Eu^{3+}$  (5 a/o) film deposited at  $500^\circ C$ . Characteristic peak associated to CTB transition (257 nm) is shown,  $\lambda_{em} = 612$  nm.

These spectra are composed by five bands corresponding to transitions from  $^5D_0$  to  $^7F_j$  ( $j=0, 1, 2, 3, 4$ ) states, respectively. The electrical dipole transitions  $^5D_0 \rightarrow ^7F_2$  at 612 nm and  $^5D_0 \rightarrow ^7F_4$  at 693 nm are the strongest emissions band observed, in agreement with the Judd-Ofelt selection rules for these transitions [11]. It is also observed a concentration quenching if the activator concentration increases above the optimum concentration, i.e. 5 a/o in the spraying solution (1.28 a/o, as measured by EDS, see Table I). Presumably, this concentration quenching is due to clusters of activators, which play the role of the killer site. In addition, the quenching occurs by energy migration through the lattice [12].

PL and CL measurements as a function of the  $T_s$  also were carried out. It was found that 612 nm emission intensity increases as  $T_s$  is increased. For lack of space, these results are not shown, and detailed studies will be published later.

The CL spectra as a function of activator concentration in the spraying solution are shown in Fig. 4. All bands produced by the  $^5D_0 \rightarrow ^7F_j$  transitions are

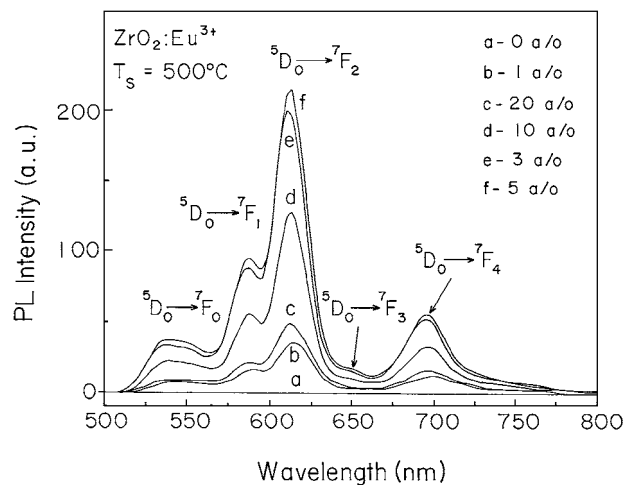


Figure 3 The PL emission spectra for  $ZrO_2:Eu^{3+}$  films as a function of the activator concentration in the spraying solution,  $\lambda_{ex} = 257$  nm.  $T_s = 500^\circ C$ .

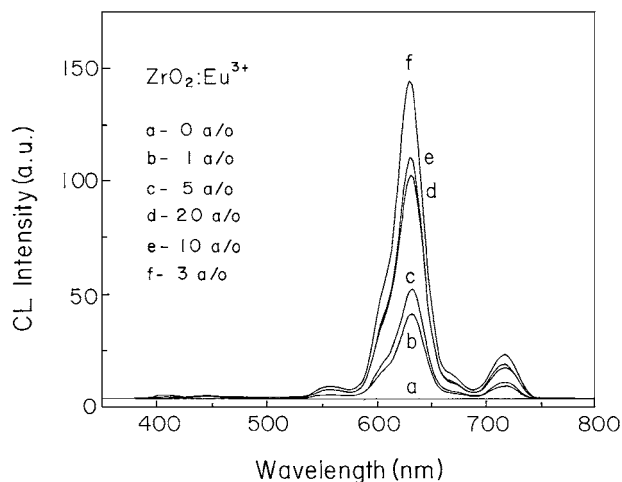


Figure 4 CL spectra for  $\text{ZrO}_2:\text{Eu}^{3+}$  films as a function of the activator concentration, under 14 kV electron accelerating potential.  $T_s = 500^\circ\text{C}$ .

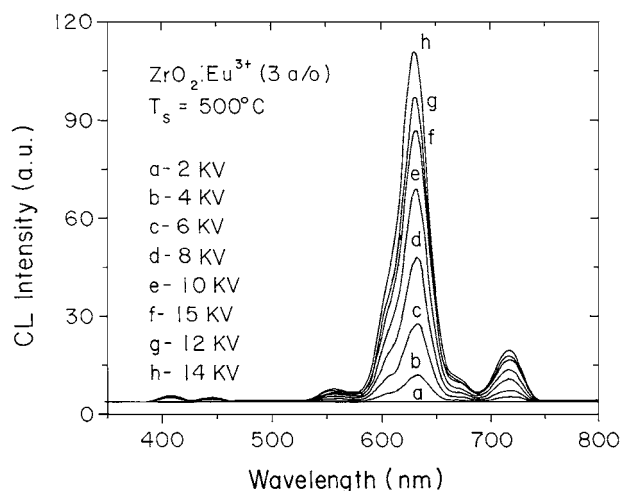


Figure 5 CL spectra of  $\text{ZrO}_2:\text{Eu}^{3+}$  (3 a/o) film as a function of the electron acceleration voltage.  $T_s = 500^\circ\text{C}$ .

shifted to lower energies; the higher peak is located at 627 nm. The maximum intensity emission is observed for 3 a/o of europium ions in the spraying solution (0.93 a/o, as measured by EDS). A concentration quenching of the CL emission is also present in this case. The accelerating voltage was 14 kV.

Fig. 5 shows plots of CL spectra measured under steady-state excitation with an accelerating beam voltages ranging from 2 kV to 15 kV. The spectra consist of the five bands typical of the  $\text{Eu}^{3+}$ , occurring within the 4f shell. A quenching of the CL emission as a function of the accelerating potentials is observed. The 14 kV

electron accelerating voltage produced the maximum CL emission.

The pyrosol technique was used to deposit, for the first time,  $\text{ZrO}_2:\text{Eu}^{3+}$  luminescent films. The films are polycrystalline and present the amorphous or tetragonal-cubic phase, depending on  $T_s$ . The luminescence emission observed is characteristic for the Eu (III). A concentration quenching was observed for PL and CL; it is shown that the optimum Eu (III) concentration for the  $^5\text{D}_0 \rightarrow ^7\text{F}_2$  transition is lower for cathode-ray excitation than for photoexcitation. It is clear that zirconia films make interesting and efficient host for  $\text{Eu}^{3+}$ . Furthermore, the location of the main emission (612 nm) is adequate for its application as good red phosphor.

### Acknowledgments

Special thanks to L. Baños and J. Guzmán for XRD and EDS measurements, respectively.

### References

1. J. C. VIGUIE and J. SPITZ, *J. Electrochem Soc.* **122** (1975) 585.
2. M. LANGLET and J. C. JOUBERT, in "Chemistry of Advanced Materials" (Blackwell Science, Oxford, England, 1993) p. 55.
3. Y. H. SOHN, R. R. BIEDERMAN and R. D. SISSON, JR., *Thin Solid Films* **250** (1994) 1.
4. R. DI MAGGIO, L. FEDRIZZI, S. ROSSI and P. SCARDI, *ibid.* **286** (1996) 127.
5. E. T. KIM and S. G. YOON, *ibid.* **227** (1993) 7.
6. A. DUPARRE, E. WELSCH, H. G. WALTHER, N. KAISER, H. MUELLER, E. HACKER, H. LAUTH, J. MEYER and P. WEISSBRODT, *ibid.* **187** (1990) 275.
7. X. D. XU, R. E. MUENCHAUSEN, N. S. NOGAR, A. PIQUE, R. EDWARDS, B. WILKENS, T. S. RAVI, D. M. WANG and C. Y. CHEN, *Appl Phys Lett.* **58** (1991) 304.
8. J. DEXPERT-GHYS, M. FAUCHER and P. CARO, *J. Solid State Chem.* **54** (1984) 179.
9. D. VAN DER VOORT and G. BLASSE, *Chem. Matter.* **3** (1991) 1041.
10. S. GUTZOV, M. BREDOL and F. WAGGESTAIN, *J. Phys. Chem. Solids* **59** (1998) 69.
11. B. HENDERSON and G. F. IMBUSH, "Optical Spectroscopy of Inorganic Solids" (Calderon Press, Oxford, 1989) p. 401.
12. J. P. VAN DER ZIEL, L. KOPF and L. G. VAN UITERT, *Phys. Rev. B* **6** (1972) 615.

Received 2 April  
and accepted 23 July 2001